Special Section: Hydrological Observatories

Core Ideas

- Two new subcatchments are used to test the importance of lithology and land use.
- Differences in lithology and land use result in differences in soils and waters.
- Despite differences, all catchments have a shallow and a deep water table
- The relative importance of flow paths controls distinct chemistry response to discharge.
- Cross-site comparison will ultimately enable upscaling from the catchment to large scale.

L. Li and D. Xiao, Civil and Environmental Engineering, Pennsylvania State Univ., University Park, PA 16802; R.A. DiBiase, J.D. Vecchio, V. Marcon, B. Hoagland, C. Wayman, P. Silverhart, T. Russo, and S.L. Brantley, Dep. of Geosciences, Pennsylvania State Univ., University Park, PA 16802; Q. Tang, I. Szink, J. Kaye, L. Guo, H. Lin, D. Eissenstat, and M. Kaye, Dep. of Ecosystem Sciences and Management, Pennsylvania State Univ., University Park, PA 16803; Y. He and K.J. Davis, Dep. of Meteorology and Atmospheric Science, Pennsylvania State Univ., University Park, PA 16802; B. Forsythe, J.Z. Williams, D. Shapich, K.J. Davis, and S.L. Brantley, Earth and Environmental Systems Institute, Pennsylvania State Univ., University Park, PA 16802; G.J. Mount, Dep. of Geosciences, Indiana Univ. of Pennsylvania, Indiana, PA 15705; A. Dere, Geography and Geology Dep., Univ. of Nebraska, Omaha, NE 68182; K. Brubaker, Dep. of Biological and Allied Health Sciences, Bloomsburg Univ. of Pennsylvania, Bloomsburg PA 17815. *Corresponding author (lili@engr.psu.edu).

Received 31 Mar. 2018. Accepted 1 July 2018. Supplemental material online.

Citation: Li, L., R.A. DiBiase, J. Del Vecchio, V. Marcon, B. Hoagland, D. Xiao, C. Wayman, Q. Tang, Y. He, P. Silverhart, I. Szink, B. Forsythe, J.Z. Williams, D. Shapich, G.J. Mount, J. Kaye, L. Guo, H. Lin, D. Eissenstat, A. Dere, K. Brubaker, M. Kaye, K.J. Davis, T. Russo, and S.L. Brantley. 2018. The effect of lithology and agriculture at the Susquehanna Shale Hills Critical Zone Observatory. Vadose Zone J. 17:180063. doi:10.2136/vzj2018.03.0063

© Soil Science Society of America. This is an open access article distributed under the CC BY-NC-ND license (http://creativecommons.org/licenses/by-nc-nd/4.0/).

The Effect of Lithology and Agriculture at the Susquehanna Shale Hills Critical Zone Observatory

Li Li,* Roman A. DiBiase, Joanmarie Del Vecchio, Virginia Marcon, Beth Hoagland, Dacheng Xiao, Callum Wayman, Qicheng Tang, Yuting He, Perri Silverhart, Ismaiel Szink, Brandon Forsythe, Jennifer Z. Williams, Dan Shapich, Gregory J. Mount, Jason Kaye, Li Guo, Henry Lin, David Eissenstat, Ashlee Dere, Kristen Brubaker, Margot Kaye, Kenneth J. Davis, Tess Russo, and Susan L. Brantley

The footprint of the Susquehanna Shale Hills Critical Zone Observatory was expanded in 2013 from the forested Shale Hills subcatchment (0.08 km²) to most of Shavers Creek watershed (163 km²) in an effort to understand the interactions among water, energy, gas, solute, and sediment. The main stem of Shavers Creek is now monitored, and instrumentation has been installed in two new subcatchments: Garner Run and Cole Farm. Garner Run is a pristine forested site underlain by sandstone, whereas Cole Farm is a cultivated site on calcareous shale. We describe preliminary data and insights about how the critical zone has evolved on sites of different lithology, vegetation, and land use. A notable conceptual model that has emerged is the "two water table" concept. Despite differences in critical zone architecture, we found evidence in each catchment of a shallow and a deep water table, with the former defined by shallow interflow and the latter defined by deeper groundwater flow through weathered and fractured bedrock. We show that the shallow and deep waters have distinct chemical signatures. The proportion of contribution from each water type to stream discharge plays a key role in determining how concentrations, including nutrients, vary as a function of stream discharge. This illustrates the benefits of the critical zone observatory approach: having common sites to grapple with cross-disciplinary research questions, to integrate diverse datasets, and to support model development that ultimately enables the development of powerful conceptual and numerical frameworks for large-scale hindcasting and forecasting capabilities.

Abbreviations: CFEMS, Cole Farm eastern mid-slope; CFRT, Cole Farm ridgetop; CFVF, Cole Farm valley floor; CFWMS, Cole Farm western mid-slope; COSMOS, cosmic-ray soil moisture observing system; CZ, critical zone; CZO, critical zone observatory; GPR, ground-penetrating radar; LRMS, Leading Ridge mid-slope; LRRT, Leading Ridge ridgetop; LRVF, Leading Ridge valley floor; mbls, meters below land surface; SSHCZO, Susquehanna Shale Hills Critical Zone Observatory; TMMS, Tussey Mountain mid-slope.

The critical zone (CZ) is defined as the zone from the top of the vegetation canopy to the bottom of the groundwater, i.e., the zone that sustains life (Brantley et al., 2007; Grant and Dietrich, 2017). The critical zone observatories (CZOs) aim to study the structure, function, dynamics, and evolution of the CZ by facilitating the interdisciplinary collaboration and data collection required to understand the system as a whole. The Susquehanna Shale Hills Critical Zone Observatory (SSHCZO), located in central Pennsylvania, is one of the nine critical zone observatories in the United States and has been a CZO since 2007 (Supplemental Fig. S1). As discussed in Brantley et al. (2018), the footprint of the SSHCZO was expanded in 2013 from the original Shale Hills catchment (0.08 km²) to encompass the much larger and diverse watershed of Shavers Creek (163 km², hydrological unit code [HUC] 12).

Underlying this expansion from a first-order catchment to a HUC 12 watershed is a hypothesis that lithology (as expressed by the Paleozoic sedimentary rocks exposed in

Shavers Creek) plays a primary role in determining the structure and function of the critical zone. This hypothesis underlies the Critical Zone Observatory Network. Critical zone architecture is impacted by the intertwined controls of bedrock lithology and structure, topography, and legacies of past climate and land-use change (Hack, 1960; Brantley et al., 2016). Most of the natural physical, chemical, and biological structure of the critical zone arises from the interplay of (i) the rate of input of fresh bedrock through tectonic processes and its inherited material properties; (ii) the dissolution and alteration of primary minerals and the formation of porosity and permeability from interactions between rock and acidic and oxygenated surface waters; and (iii) the transport of solutes and sediments off hillslopes and into rivers. As a consequence of feedbacks among hydrologic, biologic, mechanical, chemical, and anthropogenic processes, it has been hypothesized that the resulting organization of regolith and weathered bedrock properties can be linked to spatiotemporal patterns of forcing from climate, tectonics, and lithology (Anderson et al., 2013; Brantley et al., 2013; Rempe and Dietrich, 2014; St. Clair et al., 2015; Riebe et al., 2017). The fundamental mechanisms of how lithology influences the formation of critical zone structure are, however, poorly understood across the complete hierarchy of temporal scales including millennial (Miller et al., 2013), glacial-interglacial (Del Vecchio et al., 2018), and anthropogenic timescales (Walter and Merritts, 2008).

At shorter time scales (months to decades), critical zone structure dictates how catchments process energy, water, and mass (Chorover et al., 2011; Grathwohl et al., 2013). In many locations, infiltrated meteoric water partitions into (i) interflow that drains into streams rapidly along shallow subsurface pathways, and (ii) deep groundwater flow that generally enters streams over longer time scales (Benettin et al., 2015; Brantley et al., 2017). Such flow patterns affect the connectivity of the landscape to streams, and this in turn influences the export patterns of nonreactive and reactive solutes (Jencso et al., 2009; Li et al., 2017a; Wen and Li, 2018). The linkage between the critical zone structure and function, however, is poorly understood. We don't understand the relative importance of characteristics observable at the land surface (e.g., topography and land use) vs. the belowground characteristics and structure in governing water storage, flow pathways, and solute export.

Another goal of exploring the larger footprint is to learn how to understand the CZ across a variety of spatial scales, a grand challenge in forecasting Earth system dynamics (Li et al., 2017b). In scaling up to Shavers Creek, the CZO is forced to move from the Shale Hills paradigm of "measure everything everywhere" to a new approach of "measure only what is needed" (Brantley et al., 2016). However, we do not generally know what we need to measure to predict water, energy, gas, solute, and sediment fluxes across landscapes. Upscaling to Shavers Creek represents a small but important step toward developing CZ expertise for the entire Susquehanna River Basin, the largest river basin in the Chesapeake Bay watershed in the US Mid-Atlantic region. A central hypothesis

is that the linkage between geological history, lithology, and land use for a watershed lying within one climate regime can (i) illustrate some of the first-order controls on water and water quality, and (ii) inform how to upscale our understanding of fundamental processes in small watersheds to make predictions at larger scales. Such understanding will eventually enable the projection of Earth systems into the future under changing environmental conditions (Goddéris and Brantley, 2013; Duffy et al., 2014).

To upscale to the larger watershed, we have begun to monitor the main stem of Shavers Creek while simultaneously instrumenting two new subcatchments in addition to the original Shale Hills subcatchment: Garner Run and Cole Farm. Garner Run is a pristine, forested, and sandstone-underlain site, while Cole Farm is an agriculturally cultivated site (a dairy farm) on calcareous shale. Here we describe current and ongoing research efforts and summarize our current understanding of the subcatchments in the context of the entire Shavers Creek watershed and the questions of interest to the CZO team and the broader community. In addition, we present new data for the Garner Run subcatchment and some of the first published data for the Cole Farm subcatchment. We also present some initial comparisons among Shale Hills, Garner Run, and Cole Farm subcatchments.

Subcatchment Characteristics

The Shavers Creek watershed is located in the Valley and Ridge physiographic province of the Appalachian Mountains, where folded Paleozoic sedimentary rocks exert a first-order control on landscape form. Erosion-resistant sandstones form high, continuous, linear ridgelines, whereas limestones and shale units comprise the lower intervening topography (Fig. 1). Most of the upper elevations of the watershed, where Shale Hills and Garner Run are located, are forested with intermittent roads or dwellings. Forest use is largely recreational, with managed logging and occasional dwellings or businesses. The lower elevations are generally agricultural (dairy farms, forage crops with corn [Zea mays L.] and soybean [Glycine max (L.) Merr.], and pastures), with dwellings and small rural communities with low population density. Quartzitic sandstone underlies the highest elevations of the Shavers Creek watershed, while shale formations are found at middle and lower elevations. In the lower parts of the watershed, shales become more calcareous, with some limestones mapped at the lowest elevations. The original focus of the CZO, the Shale Hills subcatchment (0.08 km²) is drained by an intermittent stream formed in steeply dipping Rose Hill shale and was described by Brantley et al. (2018).

Garner Run

Garner Run $(1.34~\rm km^2)$, located $\sim 3.5~\rm km$ north of the Shale Hills site, is a headwater subcatchment with an intermittent stream flowing parallel to a syncline fold axis of the Tuscarora formation. The Tuscarora is an erosion-resistant orthoquartzitic sandstone with minor interbedded shale units. Garner Run is characterized by hillslopes that are 5 to 10 times longer than in the shale bedrock

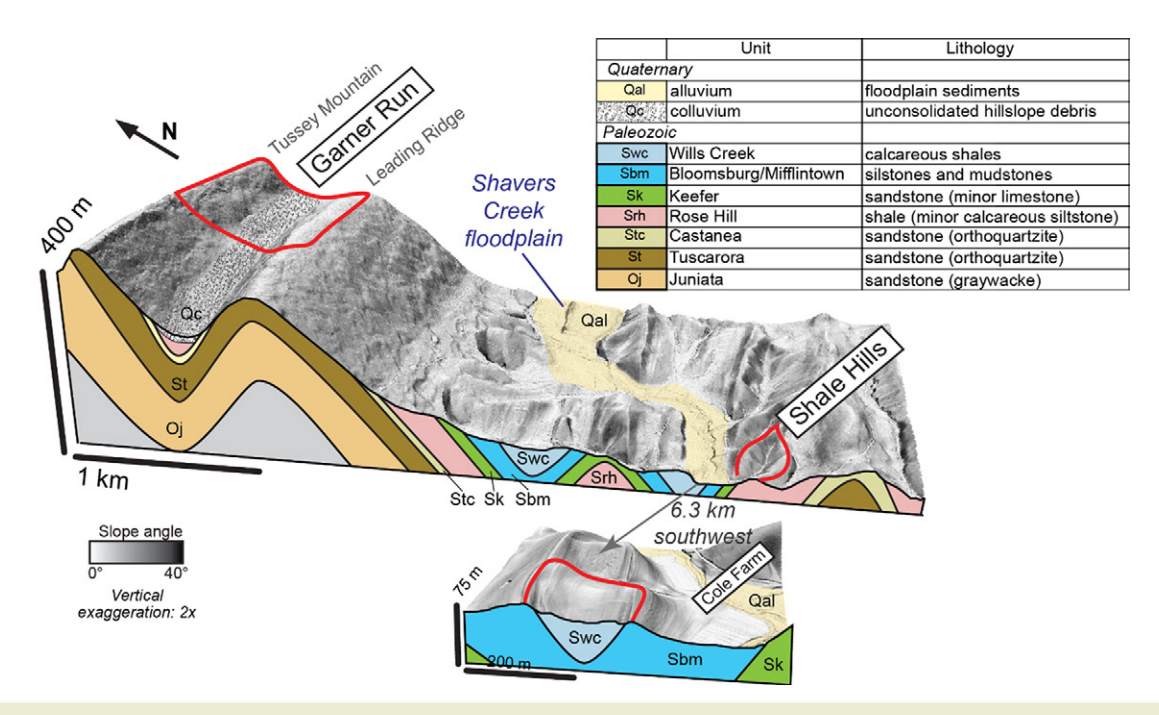


Fig. 1. Block diagram showing bedrock lithology and structure as well as surficial deposits within the Shavers Creek watershed and the three nested subcatchments. Underlying geology consists of folded Paleozoic sedimentary rocks; the Garner Run and Cole Farm subcatchments are located within synclines on sandstone and calcareous shale, respectively, whereas the Shale Hills catchment is on steeply dipping, relatively non-calcareous shale. Resistant units such as the Tuscarora and Keefer sandstones form ridges in the watershed, and shales and limestones tend to form valleys. Boulder colluvium mantles the valley axis at Garner Run, whereas alluvial deposits are located near the outlets of Shale Hills and Cole Farm.

subcatchment, with hillslopes that are not as steep as Shale Hills (DiBiase et al., 2015; Brantley et al., 2016).

Due to its location just south of the greatest extent of ice during Quaternary glaciation in Pennsylvania during the Last Glacial Maximum, surficial geology at Garner Run is largely controlled by periglacial landscape alteration (Braun, 1989; Ciolkosz et al., 1990). Supplemental Fig. S2 shows a conceptual cartoon that sketches the geomorphological features of the surface and subsurface at Garner Run. High-resolution (1-m) lidar topography (Fig. 2A) shows spatially extensive mass wasting features such as slumps and solifluction lobes associated with thawing permafrost soils (Brantley et al., 2016; Del Vecchio et al., 2018). The Tuscarora formation characteristically produces coarse blocky debris up to 1 m in diameter that were thought to have been mobilized under Pleistocene periglacial climate conditions. These boulder-rich deposits are common both on the colluvial soils mantling the planar hillslopes of Tussey Mountain and Leading Ridge (Fig. 1 and 2B) and in a thick (>9 m) colluvial fill armoring the channel of Garner Run (Fig. 2B). Perhaps because of the nature of the regolith-bouldery colluvium vs. finer clays and clay aggregates one big difference between the Garner Run and Shale Hills subcatchments is the absence of convergent-flow swales in the quartzitic subcatchment and the prominent importance of such swales in the shale subcatchment (Brantley et al., 2016).

Subsurface Structure

The stratigraphy of the colluvial valley fill in Garner Run is constrained by observations from a 9-m-deep well (HV-1, see Supplemental Fig. S3) and shallow geophysical surveys (Brantley

et al., 2016; Del Vecchio et al., 2018). Ground-penetrating radar (GPR) surveys near HV-1 highlight interfingering of coarse-grained and fine-grained valley fill (Fig. 3), consistent with surficial mapping of overlapping solifluction lobes (Fig. 2A) (Del Vecchio et al., 2018). Electrical resistivity surveys highlight a contrast in subsurface material properties between clay-rich deposits in the valley bottom and more resistive material on the north-facing hillslope of Leading Ridge (Zarif et al., 2017). Cosmogenic radionuclide dating of the colluvial fill in the valley axis of Garner Run indicates long-term (>340,000 yr) storage of debris from multiple climate cycles (Del Vecchio et al., 2018).

Multi-method shallow geophysical surveys (e.g., GPR, electrical resistivity, seismic refraction) are also being pursued within the Garner Run catchment to evaluate the degree to which past periglacial processes control the subsurface architecture important for modern critical zone processes. Roughly, the geophysical approaches are consistent with observations from soil pits (see below) that highlight an upper more permeable layer of soil + colluvium + fractured weathered rock. The soil pit at the ridgetop on Leading Ridge filled with ponded water shortly after excavation, suggesting that a perched water table forms transiently at approximately the depth of the soil pits. This upper layer is probably the pathway for transient downslope flow of subsurface water that is referred to here as interflow. Interflow discharges a few meters above the stream as a perennial spring (Fig. 2B) and discharges along the valley directly into the stream itself. The stream also receives water inputs from a deeper groundwater reservoir (\sim 10%) in the valley (Hoagland et al., 2017).

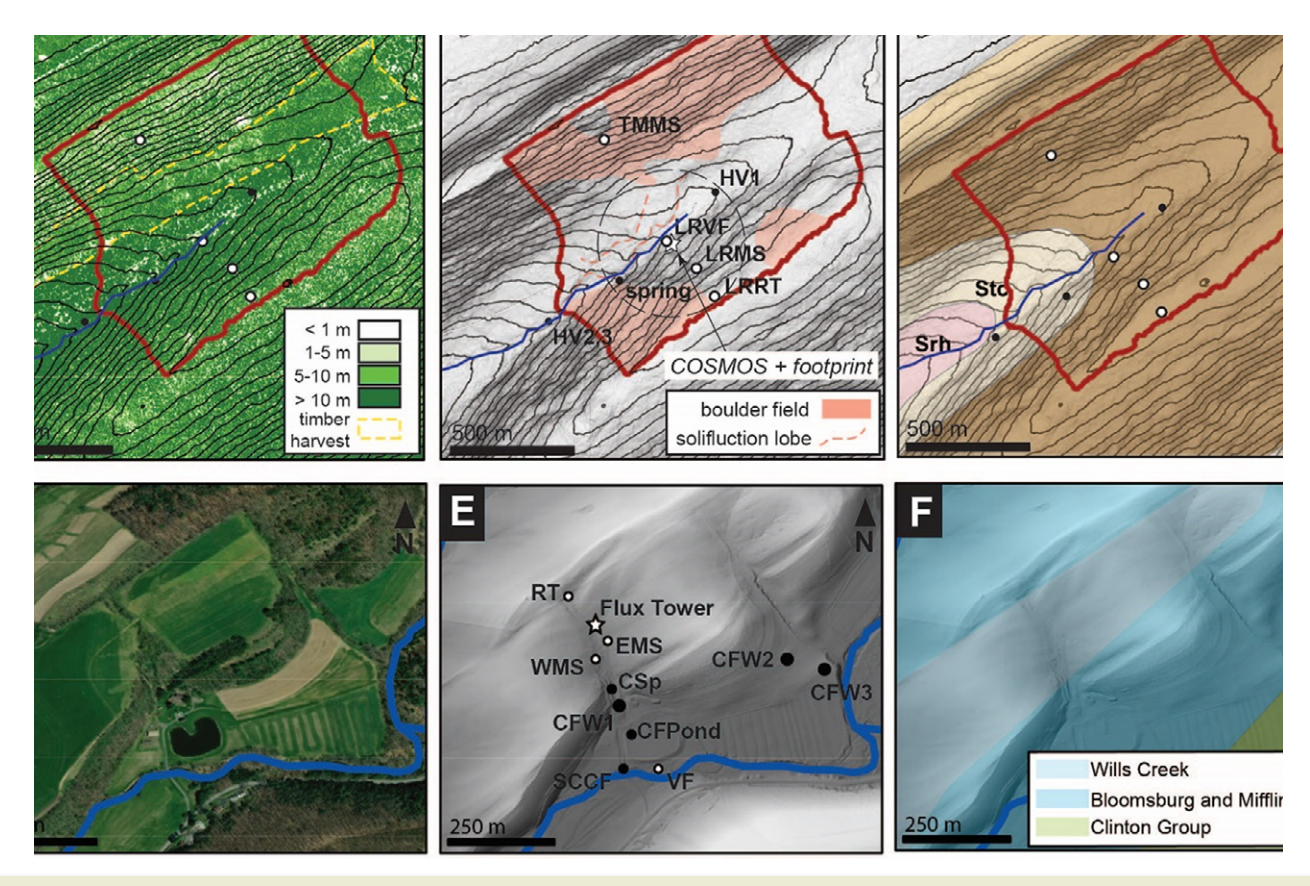


Fig. 2. Subcatchment land use, sampling locations, and lithology for (A-C) Garner Run and (D-F) Cole Farm. The Garner Run subcatchment: (A) lidar-derived canopy cover, including bare boulder patches (white) and swaths of shorter trees replanted after harvesting in the 20th century (yellow outline); (B) lidar-derived slope map with periglacial features mapped in pink and sampling locations labeled (the northern ridge is Tussey Mountain [TM] and the southern ridge is Leading Ridge [LR]; open symbols are soil pits at RT = ridgetop, MS = mid-slope, and VF = valley floor); and (C) bedrock lithology underlying the catchment including the Tuscarora orthoquartzitic sandstone (St), the Fe-cemented Castanea member of the Tuscarora (Stc), and the Rose Hill shale (Srh). The Garner Run images show the GroundHOG transect sites (white dots) and observation sites at wells and springs (black dots). Contours are 10 m. HV-1, HV-2, HV-3 are groundwater wells installed to verify the geology and investigate groundwater chemistry and flow paths. The Cole Farm subcatchment: (D) satellite image showing location of crop fields and forested sections; (E) lidar-derived slope map with sampling locations highlighted (white circles show locations of soil pits: CFRT = Cole Farm ridge top, CFEMS = Cole Farm east mid-slope, CFWMS = Cole Farm west mid-slope, and CFVF = Cole Farm valley floor; white star symbol shows the location of Cole Farm flux tower, used to collect meteorological data; and black circles show locations of water sampling sites: SCCF = Shavers Creek at Cole Farm, CFPond = Cole Farm pond, CSp = Cole Spring, and CFW = Cole Farm wells [1, 2, and 3]); and (F) lithology consists of Wills Creek formation, Bloomsburg and Mifflintown, undivided, and Clinton Group.

Lithology, Mineralogy, and Soil Properties

The hillslope soils and streambed sediments at Garner Run have lower concentrations of major elements than the soils and sediments at Shale Hills except for silica and phosphorus (Jin et al., 2010; Brantley et al., 2016; Hoagland et al., 2017). Quartz and illite clays predominate throughout the catchment, but the mineralogy differs to some extent among locations. For example, minor secondary clays such as gibbsite and mixed layer illite—vermiculite were detected in the south-facing hillslope soils and streambed sediments.

Soil pits were excavated to evaluate soils and to install instruments to monitor pore water and soil gases following the GroundHOG schema (Brantley et al., 2016). Soil pits were dug at three locations on Leading Ridge and one location on the southfacing side of Tussey Mountain. At Garner Run, depth to auger refusal (by hand) or depth to inferred bedrock (excavated with a jack hammer) in the valley floor pit ranged from 70 cm below the surface at the ridge top (LRRT) and Tussey Mountain mid-slope

(TMMS) positions to 170 cm at the valley floor (LRVF), consistent with interpretations based on GPR surveys. Mid-slope soils on the south-facing Tussey Mountain (TMMS) are developed from sandstone colluvial parent material and consist primarily of extremely gravely sandy loams (8–19% clay and 65–70% rock fragments). Ridgetop (LRRT) and mid-slope (LRMS) soils of the north-facing side of the catchment are also developed in sandstone colluvium. Soils on the Leading Ridge valley floor (LRVF) are developed from sandstone colluvium that overlies what appears to be fractured, but in place, sandstone bedrock, but it is challenging to distinguish this from boulder-rich colluvium derived from upslope (Brantley et al., 2016). Generally, soils in the Leading Ridge pits vary from extremely gravely loamy sands (8% clay and 90% rock fragments) to very gravely sandy clay loams (32% clay and 50% rock fragments) (Brantley et al., 2016; Hoagland et al., 2017).

The soil profile along the south-facing hillslope (TMMS) shows weaker horizonation than pits in the north-facing slope

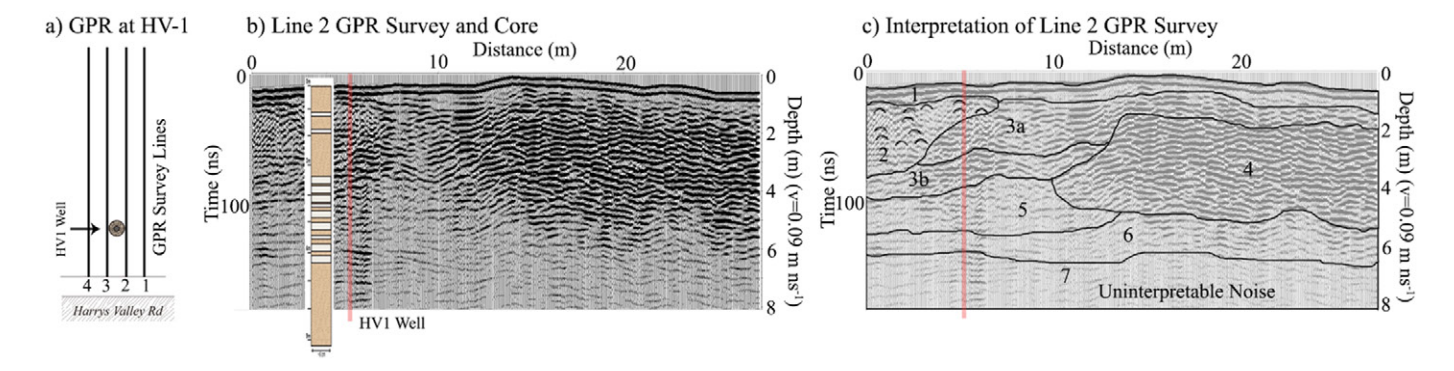


Fig. 3. (a) Schematic of time lapse ground-penetrating radar (GPR) surveys conducted at HV1 in Garner Run; (b) common offset profile along Line 2 (L2) at HV-1, with the location of the well demarcated with a vertical red line and a cartoon of the recovered core; and (c) interpreted common offset profile along L2, showing the location of HV-1 (vertical red line). Interpreted reflection Packages 1 through 7 are outlined in black; inter-package reflectors, such as diffraction hyperbola, are marked in Package 2 and coincide with quartzite clasts in a fine sand matrix. The sand matrix with isolated cobbles is present in 3a with sand content decreasing sharply at 10- to 12-m distance along the transect. In addition, sinuous parallel reflectors, interpreted as a compact zone of quartzite clasts compose Package 4 with a defined-on lap at the 3b/4 boundary. Interpretations cannot be made for Packages 1 and 7 due to ground coupling effects and low amplitude reflections or attenuation, respectively.

(LRMS) (Brantley et al., 2016), which is consistent with the higher erosion rates and sediment flux inferred for the south-facing compared with the north-facing hillsides (Del Vecchio et al., 2018). Additionally, the south-facing slope has more evidence of relic mass wasting events indicated by geomorphic features such as solifluction lobes (Brantley et al., 2016). Brantley et al. (2016) argued that the clays in the soils do not appear to be derived from Tuscarora formation bedrock and therefore may represent residual material retained during weathering and erosion of the previously overlying Rose Hill shale formation. Alternately, non-quartz material in the soils could have derived from aeolian dust inputs (Ciolkosz et al., 1990) or from clay-rich interbeds in the Tuscarora formation (Nickelson and Cotter, 1983).

Vegetation and Land Use

Garner Run is a predominantly forested watershed with trees that regenerated after widespread tree harvesting at the beginning of the 20th century. Mature trees average approximately 90 yr in age, which is common for forests of the region due to the uniform history of logging. The temperate forest is a mixture of deciduous broadleaf species with a small component of evergreen conifers. Forest composition and biomass varies depending on the topographic position in the watershed. Using measurement surveys along transects parallel to the stream, the highest biomass was measured at the toeslope of the north-facing hillslope (191.4 Mg ha⁻¹), followed by the mid-slope $(172.6 \, \text{Mg ha}^{-1})$, and then the ridgetop. The lowest biomass was measured at the mid-slope on the south-facing hillslope (121.1 Mg ha⁻¹) (Brubaker et al., 2018). Toeslope forests are dominated by northern red oak (Quercus rubra L.), black birch (Betula lenta L.), and chestnut oak (Quercus prinus L.), while the north-facing mid-slope is dominated by black birch and chestnut oak (Supplemental Table S1). The southern ridgetop is dominated by chestnut oak, red maple (Acer rubrum L.), and eastern white pine (Pinus strobus L.), and the south-facing mid-slope by red maple, black birch, and blackgum (Nyssa sylvatica Marshall). An abundant layer

of shrubs from the family Ericaceae exists below the forest canopy. This shrub layer contributes little to the aboveground biomass $(1.4-2.3\,\mathrm{Mg\,ha^{-1}},\mathrm{depending}\,\mathrm{on}$ the topographic position); however, it plays an important role in diversifying forest structure, decreasing light transmittance to the forest floor, and providing wildlife habitat.

Rooting depths in the forest are distributed with a typical exponential decay function, with >75 to 80% of the roots within 20 cm of the soil surface, although roots deeper than 1 m can be found. Moreover, the hillslope position has little effect on the relative vertical distribution of roots at Garner Run. Figure 4 compares the absolute number of root intersections per square meter in Garner Run with Shale Hills. The root intersections were measured using high-definition photographs of the root pit walls using an Olympus Stylus TG-860 Tough camera (Olympus Corporation) and custom-made mount. The absolute root distribution was determined by counting every root intersection of an imaginary plane in transects of 10 by 30 cm. This is proportional to root length density assuming that roots are randomly

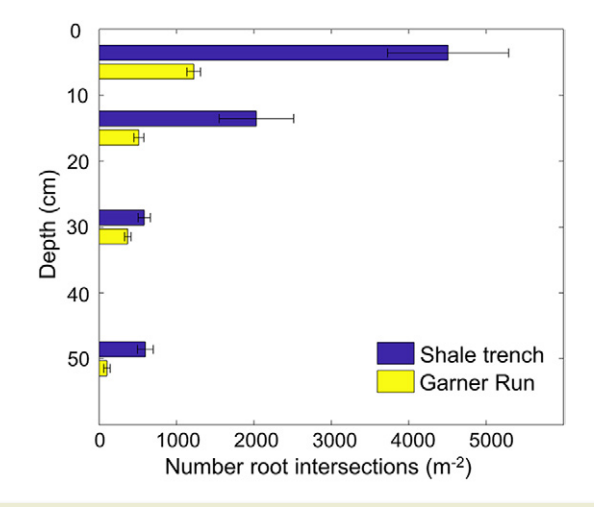


Fig. 4. Depth distribution of root intersections in the Garner Run and Shale Hills subcatchments.

distributed (Böhm, 1979). The values are averages of eight transects in each pit for three pits at each landscape position (valley floor, mid-slope, and ridgetop). The numbers indicate that Shale Hills in general has much more dense roots than Garner Run even if we assume that the rock areas (\sim 45%) have the same density of tree roots as rock-free areas. In addition, the proportion of total roots observed that were deeper (>20 cm) was higher in Garner Run than in the Shale Hills transect.

Soil Gases

We have monitored soil pCO $_2$ at Garner Run since 2015 at all GroundHOG sites using soil gas access tubes (Brantley et al., 2016) from three depths: 20, 40, and D-20 cm, where D is the interface between mobile soil and fractured rock and D-20 is 20 cm up from the bottom of the pit (Fig. 5). The patterns in soil pCO $_2$ at Garner Run largely conform to patterns identified with more intensive measurements at Shale Hills in terms of gradients with depth, seasonality, and topography (Hasenmueller et al., 2015). As expected, soil pCO $_2$ increases with depth, and the depth distribution of high pCO $_2$ is seasonally dependent. In summer, presumably due to high biological activity, soil pCO $_2$ is >10,000 μ L L $^{-1}$, even at the 20-cm depth, at all Leading Ridge sites. In fall and spring, the maximum pCO $_2$ is much lower, with concentrations

 ${<}5000\,\mu L\,L^{-1}$ often extending below 40 cm. These depth and seasonal patterns are influenced by topography. In soils where water flow is convergent (e.g., the valley floor), the deep soils always show pCO₂ >20,000 μ L L⁻¹, while such high concentrations are only rarely observed (midsummer) at ridgetop and mid-slope positions. Even in shallower layers (e.g., 20 cm), the valley floor typically had greater soil pCO₂ concentrations than the same depth in the midslope or ridgetop positions. This may indicate that soil microbial activities and root respiration are higher in relatively wetter soils in the valley floor and areas with convergent flow. Interestingly, the Leading Ridge mid-slope tends to have higher pCO₂ at a given depth than the Tussey Mountain mid-slope. This pattern may be related to differences in soil texture between the Leading Ridge hillslope (more fine-grained soils) and Tussey Mountain hillslope (more coarse-grained soils) (Del Vecchio et al., 2018). Preliminary data analysis suggests that lithological effects on pCO2 are much weaker than the depth, season, and topographic gradients described above. We will test this hypothesis further by adding pCO₂ measurements at Cole Farm in the coming growing season.

Cole Farm

The Cole Farm catchment (0.65 km²) is located \sim 4 km southwest of the Shale Hills site, draining transverse to a

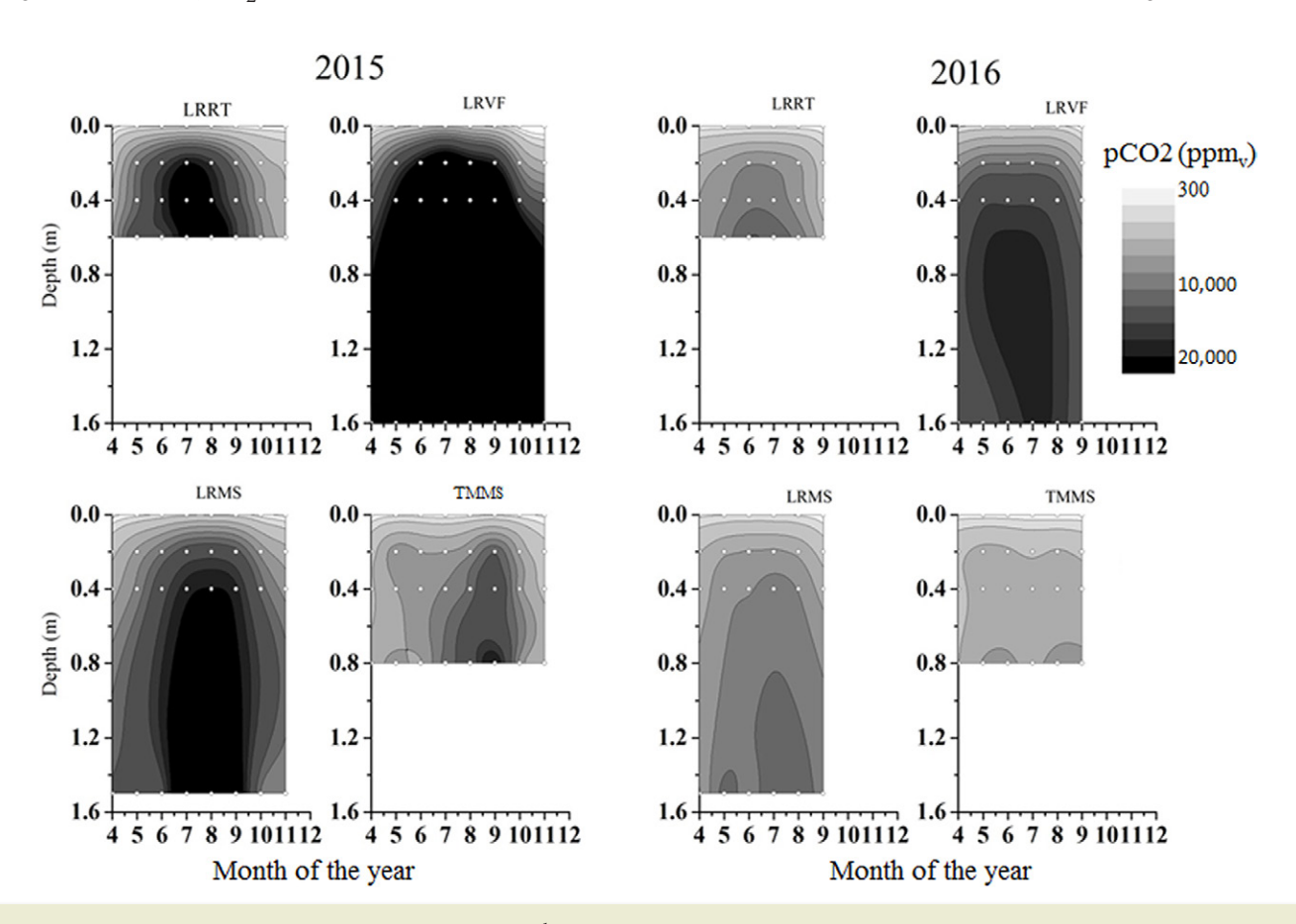


Fig. 5. Contour plots of monthly soil pCO_2 (ppmv = μL L^{-1}) as a function of soil depth (m) in the Leading Ridge ridgetop (LRRT), mid-slope (LRMS), and valley floor (LRVF) and the Tussey Mountain mid-slope (TMMS) soil pits at Garner Run in 2015 and 2016. The figure shows the change in CO_2 concentration with time by the depths of ambient (0), 20, 40, and D-20 cm depths, where D is the interface between mobile soil and fractured rock and D-20 is 20 cm up from the bottom of the pit. The values for each depth are the average of three gas tubes in each topographical position.

syncline axis of the Wills Creek formation, a calcareous shale containing interbedded siltstone, sandstone, shaley limestone, and dolomite (Fig. 1 and 2F). The date of construction of the original barn at Cole Farm was 1814, which is also estimated as the start of cultivation. This area was settled slightly later than some other regions in Pennsylvania. Surrounding farms often show a few 1- to 2-m-deep gullies; however, these features are absent at Cole Farm. This may be related to the no-till practices that were adopted at the site in the early 1900s (H. Cole, personal communication, 2018). Episodic soil loss is still observed from cultivated hillslopes during small to moderate storms, perhaps explaining the accumulation of thin soil drapes at toeslope locations. The axial channel of the Cole Farm catchment flows over a thick (>4 m) package of sediment in the valley floor. It is unclear whether these valley deposits integrate Pleistocene climate signals as in Garner Run (Del Vecchio et al., 2018), represent legacy sediments associated with centuries of agricultural land use (Walter and Merritts, 2008), or reflect intermediate timescales of hillslope-channel coupling as in the Shale Hills catchment (West et al., 2013). Along lower elevations of the farmed field, three wells (CFW1, CFW2, and CFW3) were drilled (Fig. 2E). The lithology of the wells at different depths is depicted in Supplemental Table S3.

Cole Farm is underlain by the Wills Creek, Bloomsburg, and Mifflintown formations (see Supplemental Table S3 for lithology of the formations). The farmland is contiguous to Shavers Creek to the south and consists from upper to lower elevations of a farmed field, a section of trees that roughly parallels the river

and demarcates the bottom of the farmed field, a gently sloping area where the house and other structures are located, and an area with an artificial pond that lies in the Shavers Creek floodplain. Much of the upper fields drain roughly parallel to Shavers Creek to a central forested swale and along the subsurface of the swale to emerge at a spring that drains down to the pond. Supplemental Fig. S4 shows the major subsurface structure features from the inversion model of an electrical resistivity tomography transect collected adjacent to the Cole Farm ridgetop (CFRT) pit across the north field ending approximately 50 m past the Cole Farm mid-slope pits.

Soil Observations

Due to limitations associated with working on an active farm, soil pits only loosely follow the GroundHOG schema: pits were excavated by hand and backhoe at the highest point of the upper ridge of the swale (CFRT) and within the swale on the western and eastern margins of the trees (Cole Farm western mid-slope [CFWMS] and Cole Farm eastern mid-slope [CFEMS]), and in the axis of the valley floor near Shavers Creek (Cole Farm valley floor [CFVF]) (Fig. 2D and 2E). After digging the pits, water ponded and actively infilled CFWMS, CFEMS, and CFVF. The CFRT soils are derived from colluvium ranging from silty clay loam to channery silty clay and overlie reddish (5YR 4/4) fractured rock ~1 m below the surface (Fig. 6E). The CFWMS and CFEMS soils are formed in colluvium and range from silt loam to gravelly clay loam and contain roots down to approximately the 1-m depth. Around the 2-m depth, CFWMS and CFEMS

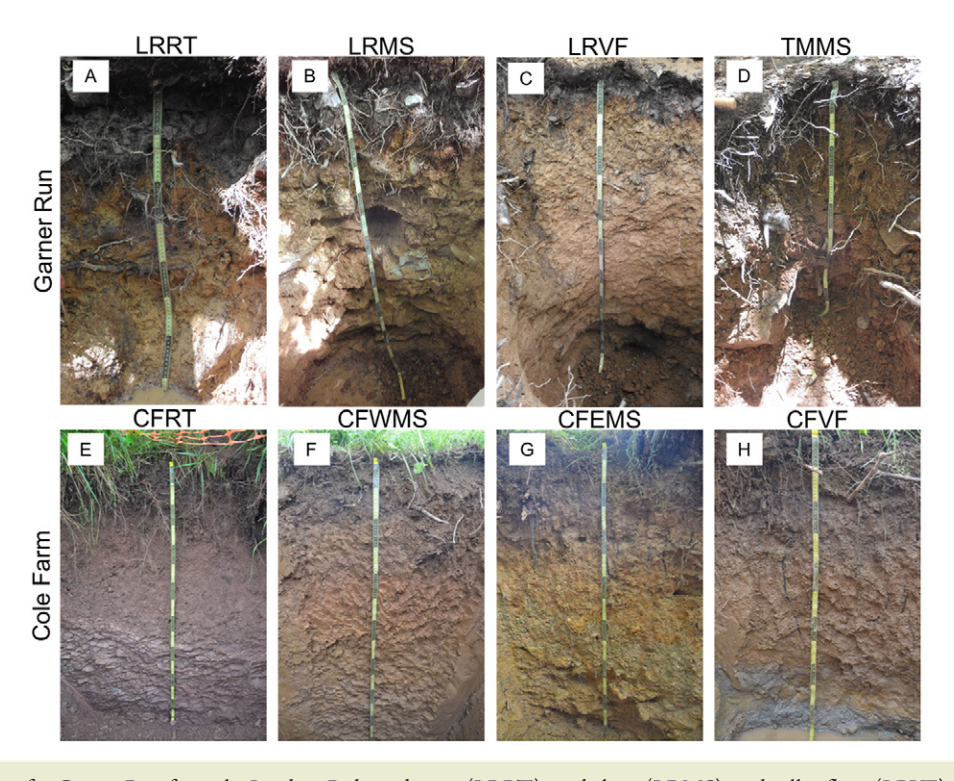


Fig. 6. Images of soil pits for Garner Run from the Leading Ridge ridgetop (LRRT), mid-slope (LRMS), and valley floor (LRVF) and the Tussey Mountain mid-slope (TMMS) and for Cole Farm from the ridge top (CFRT), west mid-slope (CFWMS), east mid-slope (CFEMS, and valley floor (CFVF). The tape measure is marked in 10-cm intervals.

contain some gravels, with possible fractured oriented parent rock at the bottom of CFEMS. The CFVF soils are derived from alluvial parent material and range from silt loam (0–0.8 m) to loam (0.8–1 m) and sandy loam (1–1.20 m), with an oxidized zone above the gleyed horizons that begin at the 0.83-m depth (Fig. 6; Supplemental Tables S4–S7). Annual crop rotations (corn and soybean) at the farm mean that roots die each year, compared with forested vegetation at Garner Run. For this reason, root surveys have not been completed on the farm field. No measurements have been made in the forested areas.

Land–Atmosphere Fluxes of Energy and Carbon Dioxide

A small tower with eddy covariance flux instruments has been installed at the downwind edge of the upper eastern hay field within Cole Farm (Fig. 2E). The system measures the exchange of water, carbon, momentum, and energy between the land surface and the atmosphere. The data from the flux tower quantify the vertical exchanges between the land surface and the atmosphere, which are often major components of the mass and energy budgets of the watershed. Monthly mean diel fluxes of latent heat (water vapor flux expressed as the energy required for the phase change of water) and CO₂ for late spring and summer of 2017 are shown in Fig. 7. The latent heat flux peaks in May and June and decreases gradually as the fall approaches. The mean monthly midday latent heat flux peaks at about 200 W m⁻², and the integrated daily evapotranspiration is 2 to 2.5 mm d^{-1} . The net ecosystem-atmosphere exchange of CO2 peaks later in the summer, with a maximum net uptake of CO2 (sum of respiration and photosynthesis) of roughly $-10 \,\mu$ mol m⁻² s⁻¹ at midday. Seasonal variability in both fluxes is relatively small. These measurements provide a valuable integral constraint on the mass and energy balances of the watershed. A complex mixture of radiative input, water availability, vegetation phenology, and plant physiology governs the fluxes.

Cross-site Comparison

Water Flow and Chemistry in Cole Farm and Garner Run

Mean annual precipitation is around 1000 mm and mean annual temperature is 10°C in central Pennsylvania (National Climatic Data Center, 2007). Stream discharge, groundwater level fluctuations, and climatic variables are fundamental measurements needed to constrain hydrologic models and mass fluxes. Precipitation data derive from the nearby Pennsylvania State University Rocks Springs Research Farm (NRCS, 2017). The streams at both catchments flow intermittently. Garner Run discharge in 2017 ranged from \sim 0 to 2.99 m³ s⁻¹, whereas discharge from Shavers Creek at Cole Farm ranged from 0.004 to 7.72 m³ s⁻¹. Base flow conditions are approximately an order of magnitude higher in Shavers Creek at Cole Farm than in Garner Run. Although the Garner Run catchment is nearly twice the size of the Cole Farm catchment, streamflow in Shavers Creek at Cole Farm was an order of magnitude greater than at Garner Run in 2017 (Fig. 8). This is because Garner Run is a first-order headwater stream, while the stream at Cole Farm represents the main stem of Shavers Creek.

The water table at Cole Farm is much deeper (2.68 to 4.45 m below land surface [mbls]) and less responsive to changes in precipitation than the Garner Run wells HV-1 (1.04–2.33 mbls) and HV-3 (0.09–0.56 mbls) (Fig. 8). Water level fluctuations in HV-3 are especially tightly coupled to diurnal and seasonal fluctuations in streamflow, as expected for an active hyporheic zone (Hoagland et al., 2017). This fast response to precipitation in Garner Run groundwater is largely attributed to the high permeability of the sands that fill the stream valley.

Above the approximate location of Cole Farm, Shavers Creek collects water discharged from predominantly forested land-scapes, while below that elevation, waters enter the creek from agricultural land and show increasing concentrations of nitrate and sulfate. Two flow paths have been inferred to enter Shavers Creek at Cole Farm: interflow in the shallow subsurface and

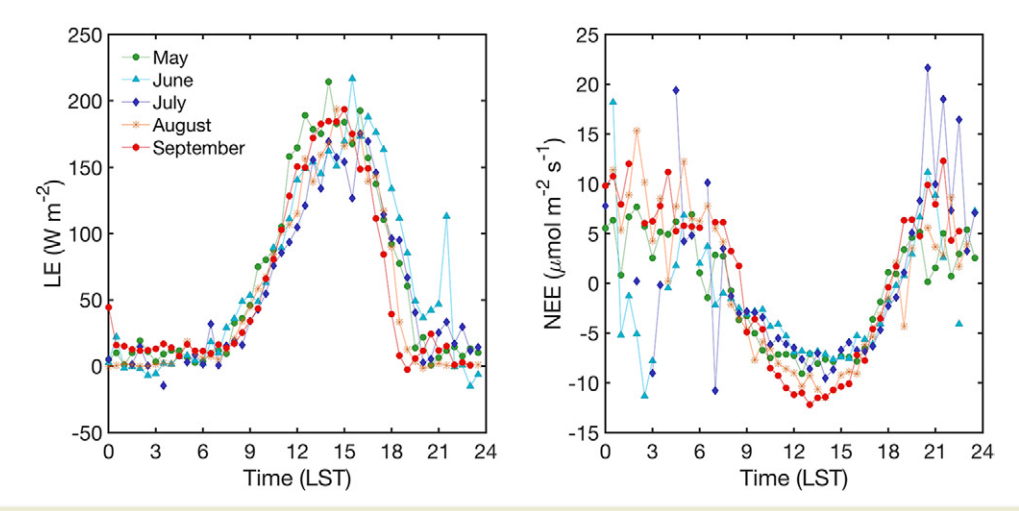


Fig. 7. Monthly average latent heat (LE) and net ecosystem-atmosphere exchange CO_2 (NEE) fluxes as a function of time in local standard time (LST) measured via eddy covariance at Cole Farm. Low friction velocity measurements ($u^* < 0.1 \text{ m/s}$) are screened; no gap filling is used. Limited nighttime data lead to high variability of the nighttime averages; LST = local standard time.

deeper flow from a regional groundwater reservoir. Nitrate and sulfate concentrations in Shavers Creek at Cole Farm are generally observed to be lower than those measured in the farm's deep groundwater as well as interflow water sampled in the spring (Fig. 2B). Like Shavers Creek at Cole Farm, Garner Run reflects a mixture of interflow and deeper groundwater (Hoagland et al., 2017). However, the interflow water sampled in the spring has lower solute concentrations than both Garner Run and the deep groundwater sampled in the valley wells. Differences between Cole Farm and Garner Run probably are related to the effects of both lithology (sandstone vs. shale) and land use (forest vs. cultivation). For example, nitrate and sulfate concentrations appear to be at least partially derived from deeper groundwaters under Cole Farm, possibly reflecting legacy effects from fertilizer inputs. Nitrate concentrations also show evidence of microbial denitrification in the pond.

Soil Moisture Comparison at Shale Hills and Garner Run Soil moisture links hydrology, geochemistry, and ecosystem processes and is one of the most extensively monitored variables in the catchments. At Garner Run, soil moisture has been measured at two different spatial scales. One is the local point measurement with frequency domain reflectometry sensors at 10, 20, and 40 cm in GroundHOG pits similar to Shale Hills (Brantley et al., 2016). The other is the areal average measurements for topsoil (\sim 10 cm) using a cosmic-ray soil moisture observing system (COSMOS) with an effective horizontal footprint of \sim 300 m (Zreda et al., 2012). Frequency domain reflectometry soil moisture measurements have now commenced at similar depths at Cole Farm in upper soil pits. A COSMOS probe is being procured for measurement at Cole Farm.

Point-Based Soil Moisture. Figure 9 shows a significant difference in monthly averaged soil moisture at 10 cm in Garner Run and Shale Hills. In each catchment, the valley floor sites have the highest water content in all seasons and in both catchments, as expected, and water content is also higher in spring and winter at many locations. The Garner Run south planar ridgetop and south planar mid-slope sites are much similar (0.13–0.22 m3 m–3) to the Shale Hills LRRT and LRMS sites (0.13–0.28 m3 m–3). The water content in the north planar mid-slope at Shale Hills

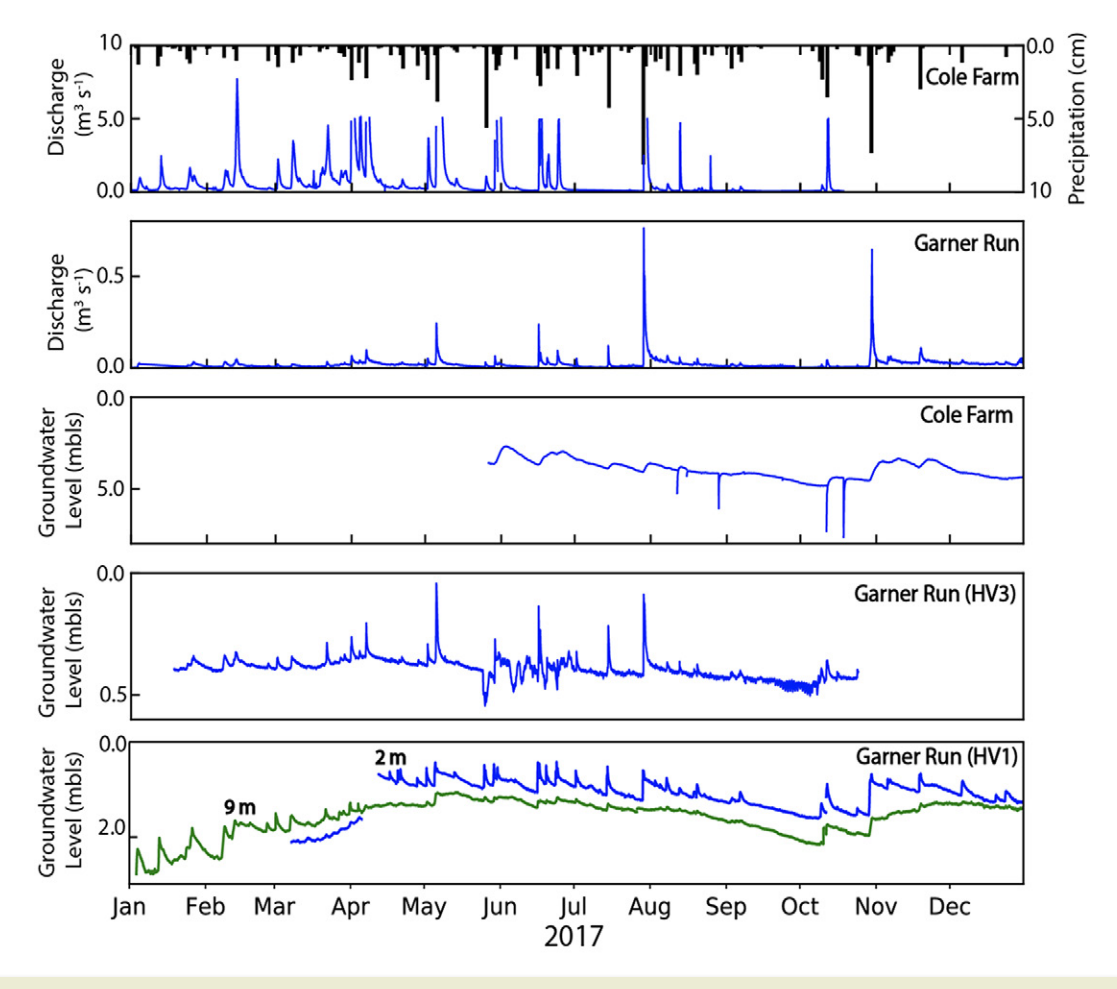


Fig. 8. Daily precipitation averages, streamflow data, and groundwater levels for the Cole Farm and Garner Run subcatchments in 2017. Groundwater levels represent the depth from the ground surface to the top of the water level (meters below land surface, mbls). Cole Farm groundwater level represents measurements made at Cole Farm Well 1 (CFW1). Groundwater levels at Garner Run represent measurements from two wells, including a nested well (HV-1) extending to 2 mbls (blue line) and 9 mbls (green line) near the mouth of Garner Run Stream, and a well \sim 0.5 m from the right bank of the stream extending 0.8 mbls near the catchment outlet (HV-3).

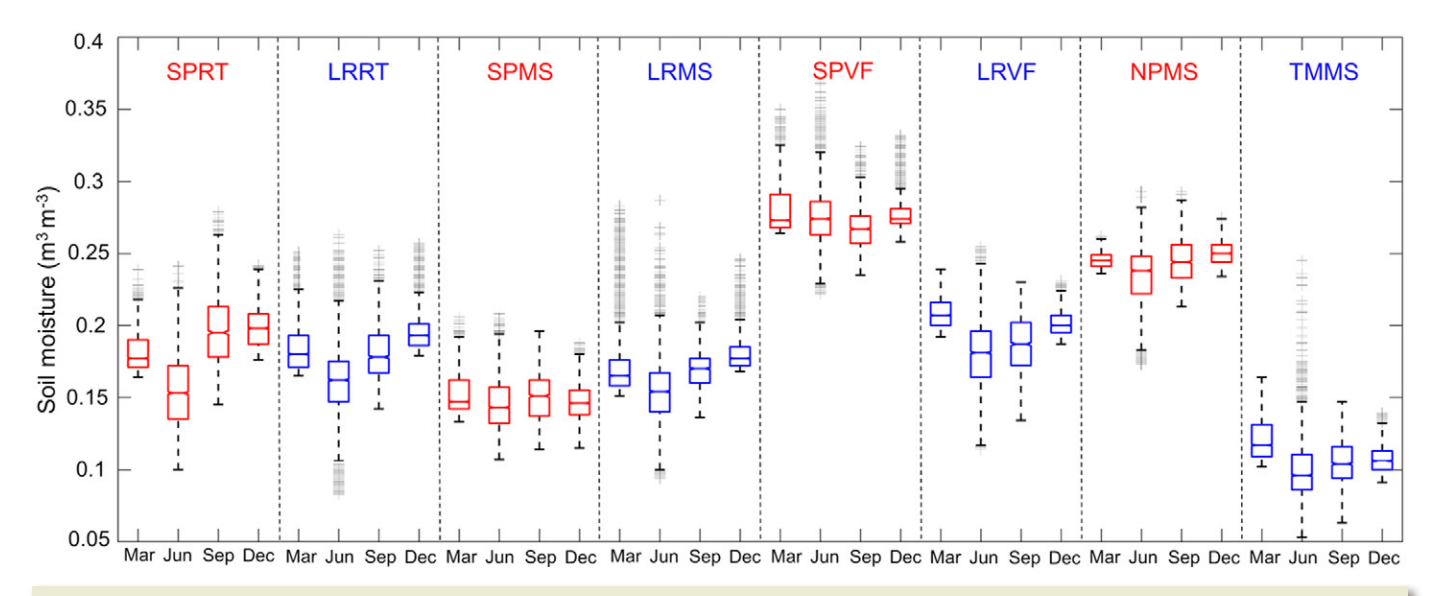


Fig. 9. Soil moisture box-and-whisker plots for GroundHOG sites at the 10-cm depth from Garner Run (Leading Ridge ridgetop [LRRT], mid-slope [LRMS], and valley floor [LRVF] and the Tussey Mountain mid-slope [TMMS] in blue) and Shale Hills (south planar ridgetop [SPRT], mid-slope [SPMS], and valley floor [SPVF] and north planar mid-slope [NPMS] in red). Seasonal trends are shown for 4 mo: March (1–31 Mar. 2017), June (1–30 June 2017), September (1–12 Sept. 2017), and December (4–31 Dec. 2017). The original data were at a 10-min time interval. In each plot, the error bars refer to the range, the rectangles refer to the 25th and 75th percentiles, the horizontal lines refer to the median values, and the gray crosses refer to the outliers.

is similar to that of the valley floor, while the water in TMMS is the lowest of all Garner Run sites. These differences are probably caused by differences in the clay content of the two sites. The sandstone-derived soil in Garner Run has 10.6% moisture content in TMMS (Brantley et al., 2016) compared with an average of 17.7% in the north planar mid-slope shale-derived soil (Liu and Lin, 2015). The low-clay soil has low water-holding capacity and therefore drains water quickly, leaving behind lower soil moisture.

COSMOS Measurements. Complementary to the point-based GroundHOG monitoring sites, COSMOS monitors neutron flux from the soils and is used to infer the areal-averaged soil

moisture. Figure 10 shows that soil moisture measured by COSMOS captures seasonal trends and responses to rainfall events. From July to September, more evapotranspiration and less rainfall lead to the longest recession period. In general, water content in the Shale Hills topsoil is higher than that in Garner Run owing to the large boulder content and more highly drained soil at Garner Run compared with the clayey soil in Shale Hills. There are a couple of occasions when Garner Run topsoil moisture is higher than that of Shale Hills. They occur in early to mid February and mid March, both in winter, that could be caused by the different snow and ice dynamics at the two subcatchments.

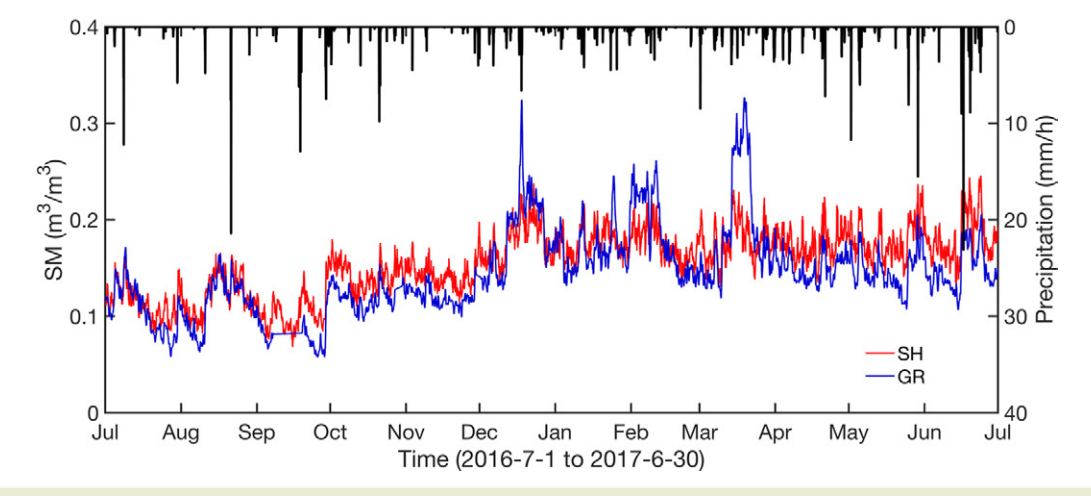


Fig. 10. Time series of soil moisture (SM) measured using a cosmic-ray soil moisture observing system (COSMOS). The data show the topsoil (<10 cm) moisture response to rainfall events. The topsoil moisture at Garner Run is generally lower than that at Shale Hills due to the larger boulder and lower clay content of Garner Run soil that leads to a greater drainage.

New Insights and Novel Scientific Findings

Geomorphology of Shale Hills and Garner Run

A comparison of the geomorphology of the Shale Hills and Garner Run catchments provides insight into the underlying geologic controls on critical zone structure and function. First, due to differences in the local rate of base level fall, long-term (millennial) erosion rates at Shale Hills are approximately three times faster than erosion rates at Garner Run (Ma et al., 2013; West et al., 2013, 2014; DiBiase et al., 2015). This contrast in erosion rate, together with the thicker soils and colluvium present at Garner Run compared with Shale Hills, implies significantly different residence times for material in the critical zone of the two catchments. At Shale Hills, landscape form may be an equilibrium morphology that reflects the asymmetry in ongoing climate forcing (West et al., 2014). In contrast, Garner Run primarily reflects the underlying structural controls on topography (Fig. 1) and integrates multiple climate cycles.

The biggest geomorphological differences between Shale Hills and Garner Run are the age and erosion rates of the regolith. Data from West et al. (2013) show that regolith post-dates the Last Glacial Maximum; bedrock erosion rates approximate 20 m Myr $^{-1}$ at Shale Hills and surficial geomorphology is dominated by pit-and-mound features from tree throw. In contrast, at Garner run, regolith pre-dates the Last Glacial Maximum; bedrock erodes at $\sim \!\! 7$ m Myr $^{-1}$ and surficial geomorphology is the product of periglacial mass movements. In short, the data may simply show that shale erodes and weathers easily and quartzitic sandstone does not.

However, untangling the effects of structure, lithology, and base level between these two landscapes is challenging because not only are there differences in lithology but Garner Run and Shale Hill are positioned differently with respect to knickpoints. The sandstone-underlain Garner Run lies above a major knickpoint and is thus insulated so far from regional base-level change. The knickpoint is moving up the stream channel slowly because of the periglacial coarse debris (especially boulders). In contrast, Shale Hills has already adjusted to the base level change at the Shavers Creek outlet. Thus, the degree to which erosion rates are controlled by lithology vs. position with respect to readjustment to base level (i.e., above or below knickpoints) remains unclear. The Cole Farm site is graded to the same base level as Shale Hills, but variations in land use are a likely influence on centennial-scale erosion rates, adding another variable to deconvolve. Regardless, the persistence of regolith at Garner Run explains why the critical zone at this site integrates over multiple climate cycles.

Two Water Tables

Although the three subcatchments are defined by different bedrock lithologies and geomorphologic characteristics, we found evidence in each catchment of a shallow and a deep water table. The shallow, lateral flow path migrates through transient, perched saturated zones in the upper, mostly unsaturated zone of each

catchment. Interflow probably travels along fast flow paths that develop because of the presence of macropores and fractures (Sidle et al., 2000; Hattanji and Onda, 2004), as well as along the interface between low- and high-permeability zones, especially those between soil horizons and interfaces of soils and weathered bedrock (Jin et al., 2011). At Shale Hills, the interflow pathways are created by a highly permeable soil zone and surficial fractured rock overlying a zone of less fractured rock that acts as a perched aquifer (Brantley et al., 2013; Sullivan et al., 2016). Shallow-flowing waters have been found to travel through the subsurface toward the valley as interflow within a residence time of approximately 1 to 5 yr (Jin et al., 2011; Sullivan et al., 2016).

In contrast to the interflow path, we define deep groundwater as relatively older, slow-moving water flowing below the regional water table or permanently saturated zone. The residence time of the deep groundwater ranges from approximately 20 to 30 yr, as estimated using water isotopes and SF₆ tracers (Sullivan et al., 2016). The regional groundwater aquifer receives recharge in every season, with highly dampened isotope signals compared with those of shallow soil waters (Thomas et al., 2013). The relative proportions of interflow and deep flow that mix in the stream and subsurface outflow at Shale Hills varies with seasonal differences in hydrostatic head (Sullivan et al., 2016). Bromide tests in Shale Hills revealed orders-of-magnitude differences in porosity and permeability between the shallow soil zones vs. the fractured and parent bedrock. The tracer tests show long tails of bromide breakthrough and are interpreted as indicating a large immobile to mobile pore volume ratio (1.5-2) (Kuntz et al., 2011). Previous estimates attribute 80 to 90% of the streamflow to interflow contributions and 10 to 20% to groundwater contributions at Shale Hills (Jin et al., 2011, 2014; Sullivan et al., 2016; Brantley et al., 2017).

At Garner Run, shallow subsurface flow paths along the hillslopes are characterized by uneven depths to bedrock and highly permeable boulder deposits within soils, whereas the valley floor is composed of 10 to 15 m of fine-grained colluvial fill. Fast-moving subsurface flow through the bouldery soils and fractured upper layers of sandstone has been observed at other sites to eventually converge into a spring (Hattanji and Onda, 2004), as observed in Garner Run (Fig. 11). The Garner Run spring flows perennially and has unique chemical characteristics compared with the shallow groundwater, soil pore water, and rainwater chemistry (Hoagland et al., 2017). Relatively low solute concentrations measured in the spring are consistent with shallow subsurface water travel along preferential flow conduits and a relatively short residence time. Similar to estimates from Shale Hills, mass balance calculations based on the chemistry of interflow and groundwater at Garner Run indicate that interflow delivers the majority of solutes to the stream (88-99%) under all flow conditions, whereas deep groundwater discharge is a relatively minor contributor (1–12%) (Hoagland et al., 2017).

Geochemical results from Cole Farm are consistent with two water tables also (see above). For example, high nitrate concentrations in the spring compared with the groundwater are

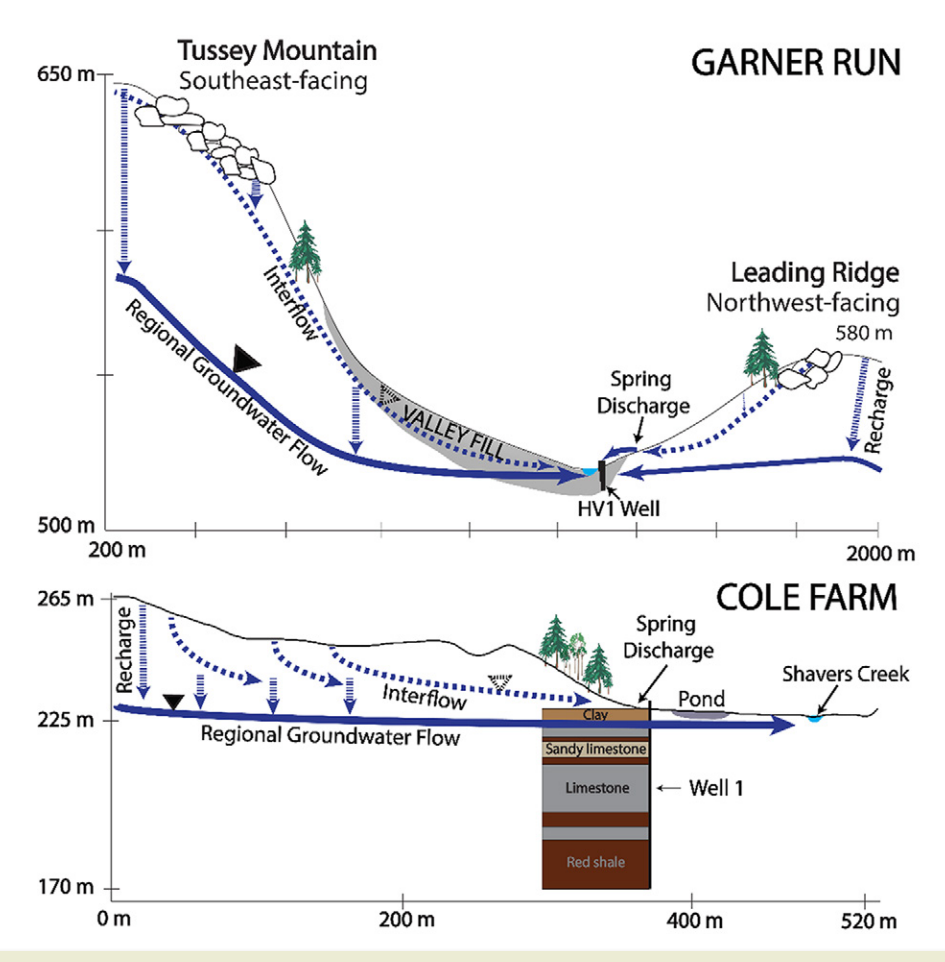


Fig. 11. Cross-section diagrams of Garner Run (top) and Cole Farm (bottom). Solid blue lines represent the regional groundwater table based on water level measurements. Dashed blue lines represent interflow pathways inferred from spring outcroppings and the depth at which the soil meets the fractured bedrock interface. Stratigraphy from Cole Farm well log data is featured to vertical scale. The stratigraphy for Garner Run in the vertical extent depicted is comprised primarily of the Tuscarora sandstone formation with <2 m of soil at the surface. The inferred extent of the valley fill at Garner Run is highlighted in gray.

consistent with a nutrient-rich surficial flow path that differs from the relatively nitrate-poor deep groundwater flow path. In contrast, sulfate concentrations in the deep groundwater at Cole Farm are higher than those measured in the spring, and we infer that sulfate in Shavers Creek is derived not only from surficial acid rain inputs but also from deeper sources such as pyrite oxidation (Brantley et al., 2013).

The presence of the two water tables across the three catchments with distinct lithologies and land uses suggests commonalities between the subsurface structure of the critical zone within the Shavers Creek watershed despite differences in topography, lithology, and land use (Herndon et al., 2015; Sullivan et al., 2016; Hoagland et al., 2017). Brantley et al. (2017) highlighted that if the advance rates of subsurface weathering fronts are equivalent to surficial erosion rates and are constant with time (e.g., steady state), then flow paths must be partitioned so that minerals with different abundances and solubilities can be removed at similar rates. At steady state (if it occurs), minerals that are highly soluble under oxic conditions such as calcite and pyrite may dissolve deep in the subsurface while less soluble minerals may dissolve at shallower depths. Furthermore, to

remove these minerals entirely from the catchment at constant rates requires less water to be partitioned to the deep reaction fronts for low-abundance, high-solubility minerals (i.e., regional groundwater flow) and more water be partitioned to shallow flow paths for higher abundance, lower solubility minerals (interflow). In addition, the steepness of the catchment must adjust to remove the entirely insoluble minerals through physical erosion at the land surface.

Concentration-Discharge Relationship

Although the proportion of interflow vs. groundwater flow contribution to the stream are similar in Shale Hills and Garner Run, the chemical signatures encoded in the concentration—discharge (C-Q) relationships at these two subcatchments differ. Here, the C-Q relationship is characterized by the slope of the logarithmic concentration (C) vs. the logarithmic discharge (Q) (Godsey et al., 2009; Musolff et al., 2015). At Shale Hills, C-Q slopes for major cations such as Mg are largely chemostatic because Mg primarily dissolves from clays in shallow soils in contact with interflow. The rates of Mg dissolution from soil clays proportionally increase as the dissolving surface area increases when the

catchment wets up. As a result, dissolution rates are high under high discharge and high water content conditions, and vice versa, leading to relatively constant Mg concentrations in the soil water and chemostatic behavior (Li et al., 2017a).

The slightly dilution-driven C-Q trends for bioactive solutes (e.g., Ca, Mn, and K) and ions that strongly complex with dissolved organic C (e.g., Fe and Al) have been attributed to the heterogeneous distribution of soil organic C (SOC), i.e., the higher SOC content in swales and the valley floor compared with planar hillslopes in Shale Hills (Herndon et al., 2015). Under dry conditions, most of the interflow comes from swales and near-valley sites with relatively high SOC. As the catchment wets up with increasing discharge from SOC-poor planar hillslopes, SOC-associated elements become increasingly diluted. This is, in fact, consistent with the conditions under which dilution behavior is observed in numerical experiments (Li et al., 2017a). Sensitivity analysis shows that dilution behavior is observed when streamflow shifts from the dominance of a chemically enriched water source under dry conditions to dilute water sources under wet, high-flow conditions.

In contrast to the dilution behavior in Shale Hills, bioactive solutes exhibit flushing behavior (e.g., C increases with increasing Q) at Garner Run. At Garner Run, this has been attributed to the storage of dissolved organic C (DOC) in the shallow hyporheic zone along the valley floor. Such flushing behavior has been widely observed for the C-Q relationship of DOC in other catchments and has been explained in the context of water dynamics and the vertical gradients of SOC in the soil (Seibert et al., 2009). That is, the rise of the water table during periods of high discharge possibly tap organic-C-rich shallow soil layers, leading to increasing DOC concentrations and organic-complexing solutes (Hoagland et al., 2017). Importantly, although both Shale Hills and Garner Run are characterized by the same sort of depth distribution of flow namely a predominant interflow path along the hillslopes that mixes with groundwater contributions to the stream in the valley—the spatial distribution of flow differs between the two subcatchments. Namely, in Shale Hills, different chemistry is generated in the convergent-flow waters in the swales than in the planar hillslopes, and mixing between these two water types is a big contributor to C-Q characteristics during high and low discharge; in contrast, no swales are observed in the Garner Run hillslopes and such patterns are not observed.

Overall, these results highlight the significant role of subsurface physical and biogeochemical spatial heterogeneities (Salehikhoo and Li, 2015; Li et al., 2011). These spatial heterogeneities regulate water flow paths and their distinct chemical signature and relative contributions to stream flow, ultimately governing stream chemistry (Miller et al., 2016; Sullivan et al., 2016).

Looking Forward

All the data from the individual subcatchments and the Shavers Creek watershed itself offer a unique interdisciplinary perspective on water, energy, gas, solute, and sediment fluxes. For

example, data from all three subcatchments led to the conceptual model of two water tables: a shallow interflow path and a deeper groundwater flow path. Traditionally, water flow paths are inferred from stable water isotopes and nonreactive solutes (McGuire and McDonnell, 2006; Rinaldo et al., 2015; Jasechko et al., 2016). However, the concurrent use of multiple datasets at the SSHCZO, including geophysical imaging, geomorphological data, and concentration-discharge relationships, identified important signatures of the routing of water that would not have been possible from the use of traditional methods alone. Clearly, such interdisciplinary datasets provide additional constraints to test conceptual models of water flow (Herndon et al., 2015; Brantley et al., 2017; Li et al., 2017a). Using the Shale Hills forested catchment as a testbed, we have developed a multiple-process-based model in the PIHM model family (Duffy et al., 2014). This includes a bedrock-to-canopy data assimilation system to integrate these fluxes into our understanding of watershed hydrology (Shi et al., 2013, 2015), a similar system for the carbon cycle (Shi et al., 2018), a landscape evolution model (Zhang et al., 2016), and the integration of reactive transport into watershed-scale hydrological processes (Bao et al., 2017). These models have emerged as useful tools to quantify the relative significance of individual processes and conditions, while at the same time assessing the integrated behavior (Heidari et al., 2017; Li et al., 2017b). This coordinated data and conceptual model development across disciplines illustrate the benefits and unique opportunities that the critical zone observatory approach offers (Baatz et al., 2018). Ultimately this will shed light on underlying principles that enables the development of powerful conceptual and numerical frameworks for large-scale hindcasting and forecasting capabilities that are of broader societal impact.

Data Management and Data Policy: Toward Collaborative Research

As outlined by Brantley et al. (2018), which introduces the Susquehanna Shale Hills Critical Zone Observatory, data collected in the SSHCZO range from Level 0 (raw data) to Level 4 (knowledge products) and are freely available to the public at http://criticalzone.org/shale-hills/data/datasets/. Supplemental Table S8 lists currently available data for Garner Run and Cole Farm. When data have not yet been processed for publication. the datasets are labeled as private, and direct requests for collaboration can be initiated. Generally, embargos on private data are less than 24 mo but may be extended up to 48 mo under special circumstances. All publications, models, and data products that make use of these datasets must include proper citation and acknowledgment. For datasets registered with doi's, the proper citation is available from the host repository (i.e., EarthChem Library, HydroShare, Dryad, etc.).

Supplemental Material

The supplemental material includes figures and tables that provide detailed information on soil descriptions, lithology, geophysical maps, vegetation sampling, available types of data, and a list of contacts for the data.

Acknowledgments

We thank Dr. Heye Bogena for handling this manuscript and two anonymous reviewers for constructive comments. Financial support was provided by National Science Foundation Grants EAR–0725019 (C. Duffy), EAR–1239285 (S. Brantley), and EAR–1331726 (S. Brantley) for the Susquehanna Shale Hills Critical Zone Observatory. Logistical support and/or data were provided by the NSF-supported Susquehanna Shale Hills Critical Zone Observatory. This research was conducted in Penn State's Stone Valley Forest, which is funded by the Penn State College of Agricultural Sciences, Department of Ecosystem Science and Management, and managed by the staff of the Forestlands Management Office. This research was conducted in Rothrock State Forest, which is funded and managed by the Pennsylvania Department of Conservation and Natural Resources, Bureau of Forestry. This research was conducted on a farm in Shavers Creek watershed at the intersection of RT 305 and Winchester Road.

References

- Anderson, R.S., S.P. Anderson, and G.E. Tucker. 2013. Rock damage and regolith transport by frost: An example of climate modulation of the geomorphology of the critical zone. Earth Surf. Processes Landforms 38:299–316. doi:10.1002/esp.3330
- Baatz, R., P.L. Sullivan, L. Li, S.R. Weintraub, H.W. Loescher, M. Mirtl, et al. 2018. Steering operational synergies in terrestrial observation networks: Opportunity for advancing Earth system dynamics modelling. Earth Syst. Dyn. 9:593–609.
- Bao, C., L. Li, Y. Shi, and C. Duffy. 2017. Understanding watershed hydrogeochemistry: 1. Development of RT-Flux-PIHM. Water Resour. Res. 53:2328–2345. doi:10.1002/2016WR018934
- Benettin, P., J.W. Kirchner, A. Rinaldo, and G. Botter. 2015. Modeling chloride transport using travel time distributions at Plynlimon, Wales. Water Resour. Res. 51:3259–3276. doi:10.1002/2014WR016600
- Böhm, W. 1979. Methods of studying root systems. Springer, Berlin. doi:10.1007/978-3-642-67282-8
- Brantley, S.L., R.A. DiBiase, T.A. Russo, Y. Shi, H. Lin, K.J. Davis, et al. 2016. Designing a suite of measurements to understand the critical zone. Earth Surf. Dyn. 4:211–235. doi:10.5194/esurf-4-211-2016
- Brantley, S.L., M.B. Goldhaber, and K.V. Ragnarsdottir. 2007. Crossing disciplines and scales to understand the critical zone. Elements 3:307–314. doi:10.2113/gselements.3.5.307
- Brantley, S.L., M.E. Holleran, L. Jin, and E. Bazilevskaya. 2013. Probing deep weathering in the Shale Hills Critical Zone Observatory, Pennsylvania (USA): The hypothesis of nested chemical reaction fronts in the subsurface. Earth Surf. Processes Landforms 38:1280–1298. doi:10.1002/esp.3415
- Brantley, S.L., M.I. Lebedeva, V.N. Balashov, K. Singha, P.L. Sullivan, and G. Stinchcomb. 2017. Toward a conceptual model relating chemical reaction fronts to water flow paths in hills. Geomorphology 277:100–117. doi:10.1016/j.geomorph.2016.09.027
- Brantley, S.L., T. White, N. West, J.Z. Williams, B. Forsythe, D. Shapich, et al. 2018. Susquehanna Shale Hills Critical Zone Observatory: Shale Hills in the context of Shaver's Creek watershed. Vadose Zone J. 17:180092. doi:10.2136/vzj2018.04.0092
- Braun, D.D. 1989. Glacial and periglacial erosion of the Appalachians. Geomorphology 2:233–256. doi:10.1016/0169-555X(89)90014-7
- Brubaker, K., Q. Johnson, and M. Kaye. 2018. Spatial patterns of tree and shrub biomass in a deciduous forest using leaf-off and leaf-on lidar. Can. J. For. Res. doi:10.1139/cjfr-2018-0033
- Chorover, J., P.A. Troch, C. Rasmussen, P.D. Brooks, J.D. Pelletier, D.D. Breshears, et al. 2011. How water, carbon, and energy drive critical zone evolution: The Jemez–Santa Catalina Critical Zone Observatory. Vadose Zone J. 10:884–899. doi:10.2136/vzj2010.0132
- Ciolkosz, E.J., B.J. Carter, M.T. Hoover, R.C. Cronce, W.J. Waltman, and R.R. Dobos. 1990. Genesis of soils and landscapes in the Ridge and Valley province of central Pennsylvania. Geomorphology 3:245–261. doi:10.1016/0169-555X(90)90006-C
- Del Vecchio, J., R.A. DiBiase, A.R. Denn, P.R. Bierman, M. Caffee, and S.R. Zimmerman. 2018. Record of coupled hillslope and channel response to Pleistocene erosion and deposition in a sandstone headwater valley, central Pennsylvania. Geol. Soc. Am. Bull. doi:10.1130/B31912.1

- DiBiase, R.A., J. Del Vecchio, and S.B. Granke. 2015. Topographic and colluvial signatures of lithology, base level, and climate in the Shavers Creek watershed, Pennsylvania. In: 2015 National Meeting Abstracts with Programs, Baltimore, MD. 1–4 Nov. 2015. Geol. Soc. Am., Washington, DC. p. 832.
- Duffy, C., Y. Shi, K. Davis, R. Slingerland, L. Li, P.L. Sullivan, et al. 2014.
 Designing a suite of models to explore critical zone function. Procedia
 Earth Planet. Sci. 10:7–15. doi:10.1016/j.proeps.2014.08.003
- Goddéris, Y., and S.L. Brantley. 2013. Earthcasting the future critical zone. Elementa Sci. Anthropocene 1:00009. doi:10.12952/journal.elementa.000019
- Godsey, S.E., J.W. Kirchner, and D.W. Clow. 2009. Concentration—discharge relationships reflect chemostatic characteristics of US catchments. Hydrol. Processes 23:1844–1864. doi:10.1002/hyp.7315
- Grant, G.E., and W.E. Dietrich. 2017. The frontier beneath our feet. Water Resour. Res. 53:2605–2609. doi:10.1002/2017WR020835
- Grathwohl, P., H. Rügner, T. Wöhling, K. Osenbrück, M. Schwientek, S. Gayler, et al. 2013. Catchments as reactors: A comprehensive approach for water fluxes and solute turnover. Environ. Earth Sci. 69:317–333. doi:10.1007/s12665-013-2281-7
- Hack, J.T. 1960. Interpretation of erosional topography in humid temperate regions. Bobbs-Merrill Co., Indianapolis.
- Hasenmueller, E.A., L. Jin, G.E. Stinchcomb, H. Lin, S.L. Brantley, and J.P. Kaye. 2015. Topographic controls on the depth distribution of soil CO₂ in a small temperate watershed. Appl. Geochem. 63:58–69. doi:10.1016/j.apgeochem.2015.07.005
- Hattanji, T., and Y. Onda. 2004. Coupling of runoff processes and sediment transport in mountainous watersheds underlain by different sedimentary rocks. Hydrol. Processes 18:623–636. doi:10.1002/hyp.1262
- Heidari, P., L. Li, L. Jin, J.Z. Williams, and S.L. Brantley. 2017. A reactive transport model for Marcellus shale weathering. Geochim. Cosmochim. Acta 217:421–440. doi:10.1016/j.gca.2017.08.011
- Herndon, E.M., A.L. Dere, P.L. Sullivan, D. Norris, B. Reynolds, and S.L. Brantley. 2015. Landscape heterogeneity drives contrasting concentration—discharge relationships in shale headwater catchments. Hydrol. Earth Syst. Sci. 19:3333–3347. doi:10.5194/hess-19-3333-2015
- Hoagland, B., T.A. Russo, X. Gu, L. Hill, J. Kaye, B. Forsythe, and S.L. Brantley. 2017. Hyporheic zone influences on concentration—discharge relationships in a headwater sandstone stream. Water Resour. Res. 53:4643— 4667. doi:10.1002/2016WR019717
- Jasechko, S., J.W. Kirchner, J.M. Welker, and J.J. McDonnell. 2016. Substantial proportion of global streamflow less than three months old. Nat. Geosci. 9:126–129.
- Jencso, K.G., B.L. McGlynn, M.N. Gooseff, S.M. Wondzell, K.E. Bencala, and L.A. Marshall. 2009. Hydrologic connectivity between landscapes and streams: Transferring reach- and plot-scale understanding to the catchment scale. Water Resour. Res. 45:W04428. doi:10.1029/2008WR007225
- Jin, L., D.M. Andrews, G.H. Holmes, H. Lin, and S.L. Brantley. 2011. Opening the "black box": Water chemistry reveals hydrological controls on weathering in the Susquehanna Shale Hills Critical Zone Observatory. Vadose Zone J. 10:928–942. doi:10.2136/vzj2010.0133
- Jin, L., N. Ogrinc, T. Yesavage, E.A. Hasenmueller, L. Ma, P.L. Sullivan, et al. 2014. The CO₂ consumption potential during gray shale weathering: Insights from the evolution of carbon isotopes in the Susquehanna Shale Hills Critical Zone Observatory. Geochim. Cosmochim. Acta 142:260–280. doi:10.1016/j.qca.2014.07.006
- Jin, L., R. Ravella, B. Ketchum, P.R. Bierman, P. Heaney, T. White, and S.L. Brantley. 2010. Mineral weathering and elemental transport during hillslope evolution at the Susquehanna/Shale Hills Critical Zone Observatory. Geochim. Cosmochim. Acta 74:3669–3691. doi:10.1016/j.gca.2010.03.036
- Kuntz, B.W., S. Rubin, B. Berkowitz, and K. Singha. 2011. Quantifying solute transport at the Shale Hills Critical Zone Observatory. Vadose Zone J. 10:843–857. doi:10.2136/vzj2010.0130
- Li, L., C. Bao, P.L. Sullivan, S. Brantley, Y. Shi, and C. Duffy. 2017a. Understanding watershed hydrogeochemistry: 2. Synchronized hydrological and geochemical processes drive stream chemostatic behavior. Water Resour. Res. 53:2346–2367. doi:10.1002/2016WR018935

- Li, L., N. Gawande, M.B. Kowalsky, C.I. Steefel, and S.S. Hubbard, 2011. Physicochemical heterogeneity controls on uranium bioreduction rates at the field scale. Environ. Sci. Technol. 45:9959–9966.
- Li, L., K. Maher, A. Navarre-Sitchler, J. Druhan, C. Meile, C. Lawrence, et al. 2017b. Expanding the role of reactive transport models in critical zone processes. Earth Sci. Rev. 165:280–301. doi:10.1016/j.earscirev.2016.09.001
- Liu, H., and H. Lin. 2015. Frequency and control of subsurface preferential flow: From pedon to catchment scales. Soil Sci. Soc. Am. J. 79:362–377. doi:10.2136/sssaj2014.08.0330
- Ma, L., F. Chabaux, N. West, E. Kirby, L. Jin, and S. Brantley. 2013. Regolith production and transport in the Susquehanna Shale Hills Critical Zone Observatory: 1. Insights from U-series isotopes. J. Geophys. Res., Earth Surf. 118:722–740. doi:10.1002/jqrf.20037
- McGuire, K.J., and J.J. McDonnell. 2006. A review and evaluation of catchment transit time modeling. J. Hydrol. 330:543–563. doi:10.1016/j.jhydrol.2006.04.020
- Miller, M.P., A.J. Tesoriero, P.D. Capel, B.A. Pellerin, K.E. Hyer, and D.A. Burns. 2016. Quantifying watershed-scale groundwater loading and instream fate of nitrate using high-frequency water quality data. Water Resour. Res. 52:330–347.
- Miller, S.R., P.B. Sak, E. Kirby, and P.R. Bierman. 2013. Neogene rejuvenation of central Appalachian topography: Evidence for differential rock uplift from stream profiles and erosion rates. Earth Planet. Sci. Lett. 369–370:1–12. doi:10.1016/j.epsl.2013.04.007
- Musolff, A., C. Schmidt, B. Selle, and J.H. Fleckenstein. 2015. Catchment controls on solute export. Adv. Water Resour. 86:133–146. doi:10.1016/j.advwatres.2015.09.026
- National Climatic Data Center. 2007. U.S. divisional and station climatic data and normals. NOAA, Natl. Climatic Data Ctr., Asheville, NC.
- Nickelson, R., and E. Cotter. 1983. Silurian depositional history and Alleghanian deformation in the Pennsylvania Valley and Ridge: 48th Annual Field Conference of Pennsylvania Geologists, Guidebook, Danville, PA. 30 Sept.–1 Oct. 1983. Pennsylvania Geol. Surv., Harrisburg.
- NRCS. 2017. SCAN site: Rock Springs, PA (SC2036). [Database.] Natl. Water and Climate Ctr., Portland, OR. https://wcc.sc.egov.usda.gov/nwcc/site?sitenum=2036&state=pa
- Rempe, D.M., and W.E. Dietrich. 2014. A bottom-up control on fresh-bedrock topography under landscapes. Proc. Natl. Acad. Sci. 111:6576– 6581. doi:10.1073/pnas.1404763111
- Riebe, C.S., W.J. Hahm, and S.L. Brantley. 2017. Controls on deep critical zone architecture: A historical review and four testable hypotheses. Earth Surf. Processes Landforms 42:128–156. doi:10.1002/esp.4052
- Rinaldo, A., P. Benettin, C.J. Harman, M. Hrachowitz, K.J. McGuire, Y. van der Velde, et al. 2015. Storage selection functions: A coherent framework for quantifying how catchments store and release water and solutes. Water Resour. Res. 51:4840–4847.
- Salehikhoo, F., and L. Li. 2015. The role of magnesite spatial distribution patterns in determining dissolution rates: When do they matter? Geochim. Cosmochim. Acta 155:107–121.
- Seibert, J., T. Grabs, S. Köhler, H. Laudon, M. Winterdahl, and K. Bishop.

- 2009. Linking soil- and stream-water chemistry based on a riparian flow-concentration integration model. Hydrol. Earth Syst. Sci. 13:2287–2297. doi:10.5194/hess-13-2287-2009
- Shi, Y., K.J. Davis, C.J. Duffy, and X. Yu. 2013. Development of a coupled land surface hydrologic model and evaluation at a critical zone observatory. J. Hydrometeorol. 14:1401–1420. doi:10.1175/JHM-D-12-0145.1
- Shi, Y., K.J. Davis, F. Zhang, C.J. Duffy, and X. Yu. 2015. Parameter estimation of a physically-based land surface hydrologic model using an ensemble Kalman filter: A multivariate real-data experiment. Adv. Water Resour. 83:421–427. doi:10.1016/j.advwatres.2015.06.009
- Shi, Y., D.M. Eissenstat, Y. He, and K.J. Davis. 2018. Using a spatially-distributed hydrologic biogeochemistry model to study the spatial variation of carbon processes in a critical zone observatory. Ecol. Modell. 380:8–21. doi:10.1016/j.ecolmodel.2018.04.007
- Sidle, R.C., Y. Tsuboyama, S. Noguchi, I. Hosoda, M. Fujieda and T. Shimizu. 2000. Stormflow generation in steep forested headwaters: A linked hydrogeomorphic paradigm. Hydrol. Processes 14:369–385. doi:10.1002/(SICI)1099-1085(20000228)14:3<369::AID-HYP943>3.0.CO;2-P
- St. Clair, J., S. Moon, W. Holbrook, J. Perron, C. Riebe, S. Martel, et al. 2015. Geophysical imaging reveals topographic stress control of bedrock weathering. Science 350:534–538. doi:10.1126/science.aab2210
- Sullivan, P.L., S.A. Hynek, X. Gu, K. Singha, T. White, N. West, et al. 2016. Oxidative dissolution under the channel leads geomorphological evolution at the Shale Hills catchment. Am. J. Sci. 316:981–1026. doi:10.2475/10.2016.02
- Thomas, E.M., H. Lin, C.J. Duffy, P.L. Sullivan, G.H. Holmes, S.L. Brantley, and L. Jin. 2013. Spatiotemporal patterns of water stable isotope compositions at the Shale Hills Critical Zone Observatory: Linkages to subsurface hydrologic processes. Vadose Zone J. 12(4). doi:10.2136/vzj2013.01.0029
- Walter, R.C., and D.J. Merritts. 2008. Natural streams and the legacy of water-powered mills. Science 319:299–304. doi:10.1126/science.1151716
- Wen, H., and L. Li. 2018. An upscaled rate law for mineral dissolution in heterogeneous media: The role of time and length scales. Geochim. Cosmochim. Acta 235:1–20. doi:10.1016/j.qca.2018.04.024
- West, N., E. Kirby, P. Bierman, and B.A. Clarke. 2014. Aspect-dependent variations in regolith creep revealed by meteoric ¹⁰Be. Geology 42:507–510. doi:10.1130/G35357.1
- West, N., E. Kirby, P. Bierman, R. Slingerland, L. Ma, D. Rood, and S. Brantley. 2013. Regolith production and transport at the Susquehanna Shale Hills Critical Zone Observatory: 2. Insights from meteoric ¹⁰Be. J. Geophys. Res., Earth Surf. 118:1877–1896. doi:10.1002/jgrf.20121
- Zarif, F., P. Kessouri, and L. Slater. 2017. Recommendations for field-scale induced polarization (IP) data acquisition and interpretation. J. Environ. Eng. Geophys. 22:395–410. doi:10.2113/JEEG22.4.395
- Zhang, Y., R. Slingerland, and C. Duffy. 2016. Fully-coupled hydrologic processes for modeling landscape evolution. Environ. Modell. Software 82:89–107. doi:10.1016/j.envsoft.2016.04.014
- Zreda, M., W.J. Shuttleworth, X. Zeng, C. Zweck, D. Desilets, T. Franz, and R. Rosolem. 2012. COSMOS: The cosmic-ray soil moisture observing system. Hydrol. Earth Syst. Sci. 16:4079–4099. doi:10.5194/hess-16-4079-2012